

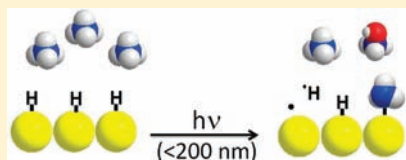
Selective, Room-Temperature Transformation of Methane to C1 Oxygenates by Deep UV Photolysis over Zeolites

Francesc Sastre, Vicente Fornés, Avelino Corma,* and Hermenegildo García*

Instituto Universitario de Tecnología Química CSIC-UPV, Universidad Politécnica de Valencia, Av. De los Naranjos s/n, 46022 Valencia, Spain

Supporting Information

ABSTRACT: Methane can directly be transformed into liquid C₁ oxygenated products with selectivities above 95% at 13% conversion by deep UV photocatalysis, in the presence of H₂O and air. Pure silica zeolites, and more specifically, beta zeolite with a large number of internal silanol groups is active and selective, while amorphous silica with no micropores is much less efficient. Irradiation produces the homolytic cleavage of surface hydroxyl groups, leading to silyloxy radicals that will generate methyl radicals from methane. The selectivity arises from the occurrence of the reaction in a confined space restricting the mobility of the radical intermediates that will be mostly attached to the solid surface. Energy consumption of the process is in the order of 7.2 Gcal × mol⁻¹ that compares very favorably with the energy required for transforming methane to synthesis gas (15.96 Gcal × mol⁻¹).



INTRODUCTION

Methane is the major component of natural gas and the most abundant feedstock.^{1–4} One of the main problems encountered in the current exploitation of natural gas is that reserves are generally in remote places and to be processed it has to be transported as compressed gas over long distances. Currently, methane is directly used in power plants, in refineries to produce H₂ by methane reforming, and to produce synthesis gas for methanol production or to feed Fischer–Tropsch units.^{5–11} It would be of much interest to directly convert methane into liquid fuels and particularly into methanol and C₁ oxygenates.

Most of the work related to the direct conversion of methane into liquid fuels involves catalytic reactions that are carried out at temperatures well above 500 °C. The three major novel processes currently under investigation are methane aromatization with molybdenum containing zeolites,^{12,13} the oxidative coupling of methane,^{14–16} and direct oxidation of methane into methanol.^{17–19} Although significant advances have been made in these processes, product selectivity, or catalyst life are still important issues to be solved.^{1,12,13,20}

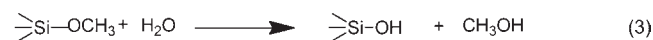
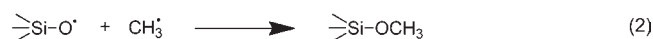
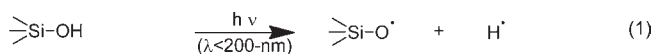
It is possible to functionalize alkanes (methane), even at room temperature, in the gas phase by means of a radical chain mechanism mediated by hydroxyl radicals.^{21–24} Unfortunately, such a process results in a very low selectivity, giving rise to extremely complex mixtures.^{21–24} The reason for this poor selectivity is that as the reaction progresses, the primary oxygenated products are more reactive than methane and undergo a network of undesired secondary reactions.

In the present work we report an original photocatalytic process that converts methane into C₁ oxygenates at room-temperature based on deep UV irradiation ($\lambda < 200$ nm) of methane in the confined spaces of zeolites containing internal OH groups in the presence of some oxygen. In this way C₁ oxygenates are obtained with 95% selectivity at a methane

conversion level of 13% in minutes. Interestingly the energy required for 13% methane conversion is one-half of the current energy used for the industrial conversion of methane to syn gas.

RESULTS AND DISCUSSION

Chemistry of the Process. The present process for room temperature methane activation is based on the general ability of hydroxyl radicals to activate methane. However, to avoid the low selectivity associated to hydroxyl radicals in the gas phase, the (hydr)oxyl radicals generated are attached to a solid surface in a confined micropore system, scavenging the initial methyl radicals to disfavor consecutive reactions. Our process involves the synthesis of zeolites with a large number of internal silanol groups (and possible coadsorbed water). When the zeolites are subjected to deep UV irradiation (165 or 185 nm), there is a homolytic cleavage of O–H bonds generating a hydrogen atom and a surface bound silyloxy radical (and hydroxyl in case water is present). Our hypothesis is that the surface bound silyloxy radicals shown in eq 1 should also be able to abstract a hydrogen atom from methane to form methyl radicals or to couple with methyl radicals to form silyl methyl ethers (eq 2) as it was known to occur for free OH· radicals in the gas phase.



While O–H chromophores are transparent to visible and UV irradiations, these O–H groups attached to the zeolite exhibit

Received: May 18, 2011

Published: September 22, 2011

Table 1. Analytical and Textural Properties of the Zeolites Used in the Present Work

zeolite	Si/Al	pore size (Å)	surface area (m ² /g)	pore volume (cm ³ /g)	population of silanol groups ^a
silica	∞	no micropores			100
silicalite	∞	5.5 × 5.1	386	0.203	10
beta (Si,F)	∞	7.1 × 6.6	481	0.22	20
beta (Al, F)	22		503	0.23	22
beta (Si,OH)	∞		490	0.22	33
beta (Al, OH)	22		540	0.24	30
commercial beta	12.5		607	0.17	31

^aRelative population of silanol groups.

a high absorption coefficients for wavelengths below 200 nm, the limit of the UV region. Therefore, it is possible to activate photochemically surface OH groups by irradiation at wavelengths shorter than 200 nm (deep UV). Prior work has reported that the direct photolysis of water by irradiation with deep UV generates hydroxyl radicals with a quantum yield approaching unity.²⁵ If this is so, we can then assume that eq 1 will also occur with high quantum yields. In a preliminary test of the concept, irradiation of the zeolite has led to the detection of hydrogen in the gas phase, thus, providing experimental support to the occurrence of such a photochemical homolytic O–H cleavage.

Nature of the Catalyst. To prove this novel concept of deep UV functionalization of methane in a confined space, a series of six zeolites was selected. The set of samples includes two different structures (medium and large pore) containing or not framework aluminum and varying the population of internal silanol groups. A nonporous amorphous silica was used for comparison purposes. Then, their activity and selectivity for the photochemical functionalization of methane into C1 oxygenates was tested. The characteristics of the different zeolites used in this work are presented in Table 1. In this Table 1, beta zeolite samples have been denoted indicating the presence or absence of framework Al and the nature of the mineralizing agent.²⁶ Notice that the 12 membered ring large pore zeolite (beta) has been synthesized with two different mineralizing agents (F⁻ or OH⁺). In the case of the beta zeolite synthesized in fluoride media the sample has lower number of hydroxyl silanol groups (see ²⁹Si MAS NMR and IR spectroscopy in the Supporting Information, Figure 1S), than the same zeolite synthesized in OH⁻ media (Supporting Information, Figure 1S). A second type of hydroxyl groups, that is, bridging ≡Al(OH)Si≡ hydroxyls, have also been generated in a Beta zeolite synthesized in OH⁻ media, by introducing Al in framework positions (see Supporting Information, Figure 2S). With the materials prepared we should be able to explore the potential role of the pore/cavities size, the influence of the number of “active sites” (hydroxy groups), as well as the impact of the different OH (bridged and silanols) types on activity and selectivity of the photocatalyst for methane transformation by deep UV irradiation.

Deep UV Photolysis. Control experiments revealed that almost negligible conversion takes place upon deep UV irradiation in the absence of any solid in a chamber saturated with water vapor.

When performing the photochemical reaction in the presence of zeolites, either in the absence or presence of oxygen, light alkanes and hydrogen are detected in the gas phase, the

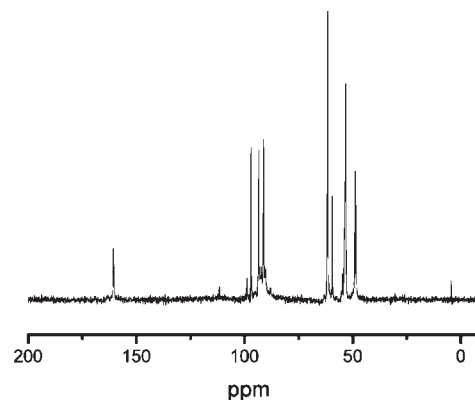


Figure 1. ¹³C NMR spectrum recorded for zeolite beta (Al, F) after 1 h 165 nm photolysis at room-temperature of ¹³C-labeled methane containing 8 vol% O₂.

difference being that the presence of oxygen reduces considerably the contribution of the products in the gas phase, decreasing the proportion of light hydrocarbons and increasing significantly the percentage of methanol and C1 oxygenates. Besides the products observed in the gas phase, a significant amount of products were also present within the pores, being the amount of the products in the gas phase very low compared to the material present in the solid (see Table 2). The total amount of organic compounds adsorbed in the catalyst after irradiation in the presence of oxygen was determined by combustion chemical analysis. Meanwhile, the nature of the products adsorbed in the solid phase was determined by MAS ¹³C NMR spectroscopy using ¹³CH₄ as substrate. A representative example of the ¹³C NMR spectra recorded for the solids after irradiation in the presence of oxygen is presented in Figure 1. As it can be seen there, in the presence of oxygen the ¹³C NMR spectra show signals corresponding to physisorbed methanol (48 ppm), methoxy groups (54 and 58 ppm) as well as formaldehyde acetals (from 97 to 99 ppm) and formic acid (168–175 ppm). The presence of adsorbed methanol and methoxysilyl groups support the mechanistic proposal based on eqs 1 and 2. Notably ¹³C NMR spectra reveal the absence of ethane and light alkanes adsorbed in the solid.

2D ¹³C NMR correlation spectroscopy confirmed that the peaks from 167 to 169 ppm assigned to formic acid are not associated to any methyl group. On the other hand, the fact that the peaks at δ about 55 ppm correspond to methyl groups was confirmed by recording off-resonance ¹³C NMR spectra and observing quartets because of the residual coupling with

Table 2. Activity Data and Product Distribution Observed after 5 min for the Room-Temperature 185 nm Photolysis of Methane and 20 vol % Oxygen in the Presence of Silicates

solid	silica gel	silicalite	beta (Si F)	beta (Al F)	beta (Si OH)	beta (Al OH)	no catalyst
total conversion (%) ^a	0.50	0.85	0.86	1.63	2.01	1.66	0.49 ^b
percentage in the solid phase	82	91	99	>99	>99	98	0
products in the gas phase (%)							
C ₂	54.2	53.3	--	--	--	84.2	73.5
H ₂	29.1	8.9	20.7	100	100	15.8	3.8
CH ₃ OH	--	37.8	79.3	--	--	--	5.1
products in the solid phase (%)							
formic acid	19.6	15.9	23.8	25.8	21.2	16.4	23.9
formaldehyde	28.3	37.6	25.5	24.4	30.8	28.7	25.8
methanol	52.1	46.5	50.7	49.8	48.0	54.9	50.3

^a Mass balances were higher than 95% The initial methane amount in these experiments is 3.7 mmol. ^b Mass balance of 85%

three protons. Furthermore, ¹³C NMR spectroscopy clearly proves that in the presence of some oxygen, the selectivity toward methanol and oxygenates is over 99% at conversions over 10%, a value that is remarkable and without precedent. Accordingly, the percentage of oxygen in the gas phase decreases from the initial 8% to 6%, indicating that some oxygen is consumed during the photolysis

The advantage of having a microporous system like in zeolites over a surface lacking microporosity is clearly deduced from the fact that photolysis over silica gives the lowest conversion of the series, though the amount of silanol groups is much larger on the amorphous silica catalyst. Concerning the influence of the zeolite composition and the presence of framework Al in the selectivity, ¹³C NMR spectroscopy shows that the presence of framework Al promotes over oxidation of methanol to formaldehyde and formic acid, while purely siliceous zeolites exhibit higher selectivity toward methanol at similar methane conversion.

Following the reaction mechanism presented in eqs 1–3 it appears that the larger number of internal silanol groups within the zeolite pores, the larger should be the activity for methane transformation upon methane irradiation. This can indeed be observed in the results given in Table 2 in where methane conversion follows the order beta(OH⁻) > beta(Al F) > beta(F), that it is in line with the relative amount of internal silanols within the samples. Therefore, we can already conclude that with respect to the solid catalyst, microporous materials appears to be better than amorphous silica, and among the zeolites, the larger the number of internal silanol groups, the higher the catalyst activity. If this is so, the conversion should be increased by increasing the zeolite to CH₄ ratio up to the point in which all the photons entering into the system are absorbed.

One point of concern was to determine the influence that the amount of adsorbed water may have on the product distribution arising from deep UV photolysis of methane over zeolites. Considering that zeolites tend to adsorb more water when the number of silanol groups is larger we have carried out the deep UV photolysis with ambient equilibrated hydrated Beta (Si,OH) zeolite. To address the influence of coadsorbed water, twin experiments in which Beta (Si, OH) was used in the hydrated form or after thermal dehydration were carried out. Although some minor variations in

Table 3. Methane Conversion and Other Catalytic Data As a Function of the Amount of Commercial Beta 811 Zeolite Employed as Photocatalyst for the Room-Temperature 185 nm Photolysis of Methane in the Presence of 20 vol % Oxygen after 5 min Irradiation

mass photocatalyst (g)	0.1	1	2	1 ^b
total conversion ^a ,	1.8	3.9	6.20	13
products in the gas phase (%) (less than 1% of total)				
C ₂				32.15
H ₂	100	100	100	53.12
CH ₃ OH				
products in the solid phase (%) (over 99% of total)				
formic acid	23.9	25.4	17.7	36
formaldehyde	25.8	24.3	25.8	22.5
methanol	50.2	50.3	56.5	40.5

^a Mass balances higher than 90% ^b After 1 h irradiation.

the proportion of the products adsorbed in the zeolite were observed, it is safe to say that the water content in the zeolite is not relevant at the conversion levels achieved in our experiments.

In most of the experiments carried out in the presence of oxygen the products adsorbed on the photocatalyst account for most of the 99% of all methane converted. Combustion chemical analysis to determine the carbon content of the zeolite wafers shows that the carbon content also varies depending on the zeolite structure, the irradiation wavelength, and the irradiation time. Concerning the irradiation wavelength, although selectivity and product distribution were very similar in both cases, it was found that the 185 nm setup was more efficient and higher conversions were obtained in less time and lower energy consumption than when photolysis was performed with the 165 nm system. Precedents in the literature have estimated that the quantum yield of the homolytic O–H bond breaking using photons in the deep UV region was essentially the unity²⁵ and the same can be implied here for either 165 or 185 nm, photolysis. Therefore the difference observed in our case should reflect more differences in the design of the 165 or 185 nm system than real differences in quantum yields. In addition, it was found that methane conversion increases with the amount of

photocatalyst present in the photoreactor. (See results in Table 3). This influence can be simply rationalized considering that the population of silanols needed in eqs 1–3 increases with the amount of photocatalyst. It is remarkable that methane conversions above 13% could be obtained in 1 h at 185 nm irradiation with selectivity over 99% toward oxygenated products. Blank controls consisting on the irradiation of methane in the presence of moisture-saturated oxygen atmosphere at 185 nm show negligible conversion, thus, reinforcing again the need of silanol groups to promote methane conversion.

Two-Step Cycle. On the basis of the characterization of the reaction products, it is possible to devise a two-step cycle consisting of (a) irradiation of methane over the zeolite to form oxygenated species and (b) desorption of these oxygenated compounds formed and regeneration of the

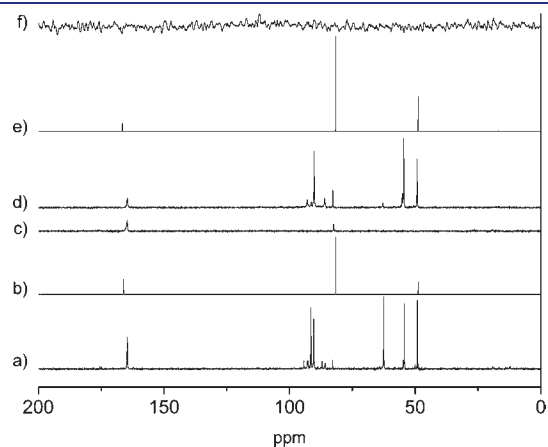


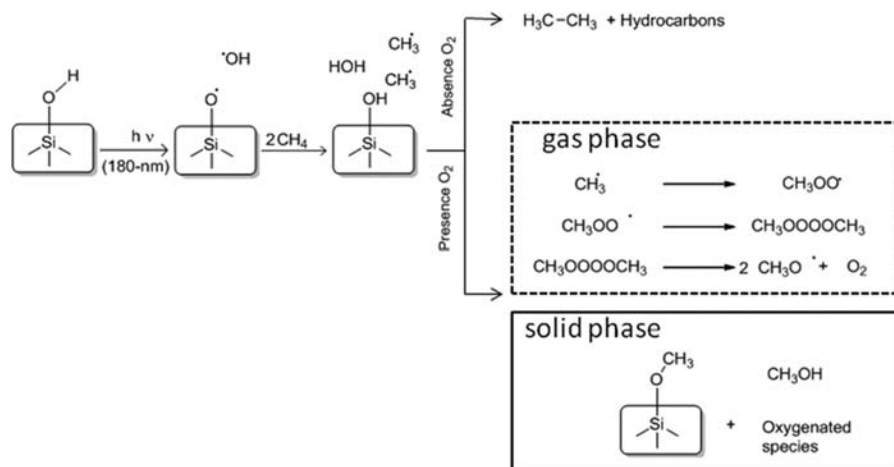
Figure 2. ^{13}C NMR spectrum recorded at room temperature for (a) zeolite beta (Si, OH) after 11 h 165 nm photolysis at room temperature of $^{13}\text{CH}_4$ containing 8 vol% O_2 , (b) room temperature spectrum of the water solution after desorbing the products at $150\text{ }^\circ\text{C}$ for 1.5 h, (c) photolyzed zeolite beta (Si,OH) after being submitted to water desorption, (d) zeolite beta (Si, OH) after a second 11 h 165 nm photolysis at room-temperature of methane containing 8 vol% O_2 , (e) room temperature spectrum of water used to desorb products at $150\text{ }^\circ\text{C}$ after 1.5 h, and (f) zeolite Beta (Si,OH) after a second water desorption.

solid. To assess the feasibility of the two-step process, the beta (Al, OH) zeolite was submitted to three cycles involving each time photolysis in a methane/air atmosphere followed by washing the solid with water to remove the adsorbed products. A summary of the MAS ^{13}C NMR spectra recorded for this series of consecutive irradiation/desorption experiments are shown in Figure 2. It can be seen there that the aqueous phase after washing the Beta (Al, OH) zeolite clearly contains methanol, formol and formic acid (spectra b and e in Figure 2), while the resultant solid is almost free of organic compounds (spectra c and f in Figure 2). In addition, these experiments also indicated that the zeolite can be reused (at least 3 times) without observing changes in the behavior of the material.

Reaction Mechanism. Concerning the reaction mechanism, we propose that deep UV irradiation will produce the homolytic splitting of silanol groups into silyloxy radicals and a hydrogen atom (Scheme 1) as it has been reported in the literature for water splitting.²⁵ These oxyl radicals will generate methyl radicals from methane as it is well-known in vapor phase radical chemistry for hydroxyl radicals. Depending on the presence or absence of oxygen these methyl radicals will evolve giving oxygenated species or hydrocarbons, respectively. Selectivity will arise from the occurrence of the reaction on a surface and in a confined space, restricting the mobility of the radical intermediates that will be mostly attached to the solid surface. As commented before, the presence of water does not influence selectivity, at least, in the range of conversion studied here. In contrast, the presence of oxygen is crucial to scavenge methyl radicals, stopping the formation of hydrocarbons (see Scheme 1).

Energy Consumption. A first calculation of the energy required for the room temperature methane activation based on deep UV photolysis over a solid support, was carried out by determining the energy consumption of the lamp to achieve a certain methane conversion. The results indicate that while the transformation of 1 mol of methane to syn gas requires about $15.9\text{ Gcal} \times \text{mol}^{-1}$,²⁷ to achieve 13% conversion using the 185 nm lamp (60 min irradiation), the energy consumption is $7.16\text{ Gcal} \times \text{mol}^{-1}$.

Scheme 1. Proposed Mechanism for the Deep UV Transformation of Methane on Silica Surface



CONCLUSIONS

Using ^{13}C labeled methane and determining the product distribution by solid state ^{13}C NMR spectroscopy, it has been shown that deep UV photolysis of methane over Beta zeolites containing internal silanol groups allows the room-temperature transformation of methane into C1 oxygenates. When a small amount of oxygen is present, the product selectivity toward C1 oxygenated products, that is, methanol, formaldehyde, and formic acid is over 95%. The nature of the zeolite plays a role in the conversion, the most appropriate material being the *all-silica* beta zeolite prepared in OH^- media to maximize the number of internal silanol groups. In addition, it has been found that the presence of coadsorbed water does not alter conversion or product distribution in the experimental range studied here. The estimated energy consumption of the process to convert one mole of methane is about one-half than the energy required for the conventional methane steam reforming process.

EXPERIMENTAL SECTION

Silica gel and the zeolites used in this work were either commercial samples (Fluka) or were synthesized following the reported procedures.^{26,28} In particular, two of the beta zeolites [beta(Al, OH) and beta(Si, OH)] were obtained by using OH^- as mineralizing agent, while two other two beta samples [beta(Al, F) and beta(Si, F)] were obtained using HF as mineralizing agent as reported.^{26,28}

The deep UV photoactivation of methane by irradiation of solid zeolite surface was performed by preparing compressed zeolite wafers that were submitted to prior dehydration by thermal treatment at 350 °C under reduced pressure and then handled under inert, dry atmosphere before irradiation. These zeolite wafers were placed in a chamber (either 116 or 260 mL capacity for the 165 or 185 nm system) that was evacuated under vacuum and refilled with methane and nitrogen (as internal standard) or methane (3 or 3.7 mmol for 165 or 185 nm irradiation) and air at 0.5 bar. The system (see Supporting Information) was submitted to irradiation with the output of a deuterium (165 nm) or mercury (185 nm) lamp and the course of the reaction followed by analysis of the gas phase and the organic compounds adsorbed in the solid. Reproducibility of the experiments was checked by performing independent experiments in quadruplicate, whereby consistent results were obtained. Analyses of the gas phase were performed by gas chromatography using thermal conductivity and flame ionization detectors.

The mass balance was determined by adding the moles of the products in the gas phase (typically low) to the moles of methane converted in the solid. Equation S1 in the Supporting Information was employed for these calculations. Considering the relatively low methane conversion, oxygen at the initial concentrations employed was never the limiting reagent.

The two steps cycle experiment were carried out using the 165 nm set up and 100 mg of zeolite beta(Si,OH) using ^{13}C labeled methane and 8 v/v % of oxygen for 11 h. After this time, the solid was submitted to solid state ^{13}C RMN spectroscopy before extracting the soluble material with 1.5 mL of D_2O placed in a autoclave at 150 °C for 1 h. Then, the suspension was cooled down at room temperature and filtered. Once the solid was dried, both the D_2O solution and the dry zeolite where submitted to ^{13}C NRM spectroscopy.

ASSOCIATED CONTENT

S Supporting Information. MAS ^{29}Si NMR spectra of beta(Si, F), beta(Si, OH), and beta(Al, OH), blank control of deep UV photolysis of commercial beta zeolite, schematic of

deep UV photoreactors and emission spectra of the lamps, and determination of the mass balances. This information is available free of charge via the Internet at <http://pubs.acs.org/>.

AUTHOR INFORMATION

Corresponding Author

acorma@itq.upv.es; hgarci@qim.upv.es

ACKNOWLEDGMENT

Financial support by the Spanish Ministry of Science and Innovation (MICINN Grants CTQ-2009-0585 and CONSOLIDER INGENIO MULTICAT) is gratefully acknowledged.

REFERENCES

- (1) Wang, H.; Liu, Z. M. *Prog. Chem.* **2004**, *16*, 593–602.
- (2) Lunsford, J. H. *Catal. Today* **2000**, *63*, 165–174.
- (3) Ashcroft, A. T.; Cheetham, A. K.; Green, M. L. H.; Vernon, P. D. F. *Nature* **1991**, *352*, 225–226.
- (4) Wang, S. B.; Lu, G. Q. M.; Millar, G. J. *Energy Fuels* **1996**, *10*, 896–904.
- (5) Armor, J. N. *Appl. Catal., A* **1999**, *176*, 159–176.
- (6) Fierro, J. L. G. *Catal. Lett.* **1993**, *22*, 67–91.
- (7) Hu, Y. H.; Ruckenstein, E. *Adv. Catal.* **2004**, *48*, 297–345.
- (8) Pena, M. A.; Gomez, J. P.; Fierro, J. L. G. *Appl. Catal., A* **1996**, *144*, 7–57.
- (9) Rostrup-Nielsen, J. R.; Sehested, J.; Norskov, J. K. *Adv. Catal.* **2002**, *47*, 65–139.
- (10) Tsang, S. C.; Claridge, J. B.; Green, M. L. H. *Catal. Today* **1995**, *23*, 3–15.
- (11) Vanhook, J. P. *Catal. Rev.—Sci. Eng.* **1980**, *21*, 1–51.
- (12) Choudhary, T. V.; Aksoylu, E.; Goodman, D. W. *Catal. Rev.—Sci. Eng.* **2003**, *45*, 151–203.
- (13) Guisnet, M.; Gnep, N. S.; Alario, F. *Appl. Catal., A* **1992**, *89*, 1–30.
- (14) Amenomiya, Y.; Birss, V. I.; Golezdzinowski, M.; Galuszka, J.; Sanger, A. R. *Catal. Rev.—Sci. Eng.* **1990**, *32*, 163–227.
- (15) Keller, G. E.; Bhasin, M. M. *J. Catal.* **1982**, *73*, 9–19.
- (16) Lee, J. S.; Oyama, S. T. *Catal. Rev.—Sci. Eng.* **1988**, *30*, 249–280.
- (17) Foster, N. R. *Appl. Catal.* **1985**, *19*, 1–11.
- (18) Gesser, H. D.; Hunter, N. R.; Prakash, C. B. *Chem. Rev.* **1985**, *85*, 235–244.
- (19) Otsuka, K.; Wang, Y. *Appl. Catal., A* **2001**, *222*, 145–161.
- (20) Ismagilov, Z. R.; Matus, E. V.; Tsikoza, L. T. *Energy Environ. Sci.* **2008**, *1*, 526–541.
- (21) Fontcave, M.; Pierre, J. L. *Bull. Soc. Chim. Fr.* **1993**, *130*, 77–85.
- (22) Basch, H.; Mogi, K.; Musaev, D. G.; Morokuma, K. *J. Am. Chem. Soc.* **1999**, *121*, 7249–7256.
- (23) Yoshizawa, K.; Shiota, Y.; Yumura, T.; Yamabe, T. *J. Phys. Chem. B* **2000**, *104*, 734–740.
- (24) Poczesniak, T.; Sobkowiak, A. *J. Mol. Catal. A: Chem.* **2003**, *194*, 1–11.
- (25) Getoff, N.; Schenk, G. O. *Photochem. Photobiol.* **1968**, *8*, 167–178.
- (26) Cambor, M. A.; Corma, A.; Valencia, S. *J. Mater. Chem.* **1998**, *8*, 2137–2145.
- (27) Worrell, E.; Phylipsen, D.; Einstein, D.; Martin, N. Lawrence Berkely National Laboratory 2000, LBNL-44314.
- (28) Corma, A.; Navarro, M. T.; Rey, F.; Valencia, S. *Chem. Commun.* **2001**, 1486–1487.